PLOS ONE

RESEARCH ARTICLE

Aquaporins are main contributors to root hydraulic conductivity in pearl millet [*Pennisetum glaucum* (L) R. Br.]

Alexandre Grondin[1,2,3,4]*, Pablo Affortit[1,2], Christine Tranchant-Dubreuil[1], Carla de la Fuente-Cantó[1], Cédric Mariac[1], Pascal Gantet[1], Vincent Vadez[1,5], Yves Vigouroux[1], Laurent Laplaze[1,2]

1 UMR DIADE, IRD, Université de Montpellier, Montpellier, France, **2** Laboratoire Mixte International Adaptation des Plantes et Microorganismes Associés Aux Stress Environnementaux, Dakar, Senegal, **3** Laboratoire Commun de Microbiologie, Dakar, Senegal, **4** Centre d'Étude Régional pour l'Amélioration de l'Adaptation à la Sécheresse, Thiès, Senegal, **5** International Crops Research Institute for Semi-Arid Tropics (ICRISAT), Hyderabad, India

* alexandre.grondin@ird.fr

Citation: Grondin A, Affortit P, Tranchant-Dubreuil C, de la Fuente-Cantó C, Mariac C, Gantet P, et al. (2020) Aquaporins are main contributors to root hydraulic conductivity in pearl millet [*Pennisetum glaucum* (L) R. Br.]. PLoS ONE 15(10): e0233481. https://doi.org/10.1371/journal.pone.0233481

Editor: Sergey Shabala, University of Tasmania, AUSTRALIA

Received: May 5, 2020

Accepted: September 11, 2020

Published: October 1, 2020

Data Availability Statement: All relevant data are within the manuscript and its Supporting Information files. All sequences and Protein Data Bank files are available at: https://dataverse.ird.fr/dataset.xhtml?persistentId=doi:10.23708/WVCG5O. All new sequences are also available from the GenBank database (accession number MT474859 for PgPIP2-8, MT474860 for PgTIP3-1, MT474861 for PgTIP4-1, MT474862 for PgTIP4-2, MT474863 for PgTIP4-3, MT474866 for PgNIP1-2, MT474867 for PgNIP3-5, MT474868 for PgSIP1-2,

Abstract

Pearl millet is a key cereal for food security in arid and semi-arid regions but its yield is increasingly threatened by water stress. Physiological mechanisms relating to conservation of soil water or increased water use efficiency can alleviate that stress. Aquaporins (AQP) are water channels that mediate root water transport, thereby influencing plant hydraulics, transpiration and soil water conservation. However, AQP remain largely uncharacterized in pearl millet. Here, we studied AQP function in root water transport in two pearl millet lines contrasting for water use efficiency (WUE). We observed that these lines also contrasted for root hydraulic conductivity (Lpr) and AQP contribution to Lpr. The line with lower WUE showed significantly higher AQP contribution to Lpr. To investigate AQP isoforms contributing to Lpr, we developed genomic approaches to first identify the entire AQP family in pearl millet and secondly, characterize the plasma membrane intrinsic proteins (PIP) gene expression profile. We identified and annotated 33 AQP genes in pearl millet, among which ten encoded PIP isoforms. *PgPIP1-3* and *PgPIP1-4* were significantly more expressed in the line showing lower WUE, higher Lpr and higher AQP contribution to Lpr. Overall, our study suggests that the PIP1 AQP family are the main regulators of Lpr in pearl millet and may possibly be associated with mechanisms associated to whole plant water use. This study paves the way for further investigations on AQP functions in pearl millet hydraulics and adaptation to environmental stresses.

Introduction

Plant hydraulics depends on soil water capture by roots, transport to the leaves and diffusion as vapor from the stomatal cavity to the atmosphere. In this plant hydraulic continuum, radial water transport from the soil solution to the xylem vessels uses two paths: the apoplastic path

MT474869 for PgSIP2-1 and MT474864 and MT474865 for TIP5-1).

Funding: This work was supported by the CGIAR Research Programme on Grain Legumes and Dryland Cereals (GLDC). PA was supported by the Cultivar program from the Agropolis Foundation as part of the "Investissement d'Avenir" (ANR-I0-LABX-0001-0I) under the frame of I-SITE MUSE (ANR-16-IDEX-0006). The French Agence Nationale de la Recherche supports the post-doctoral fellowship of CFC (ANR Grant RootAdapt n °ANR17-CE20-0022-01 to LL).

Competing interests: The authors have declared that no competing interests exist.

where water flows along the cell wall structures, and the cell to cell path where water can flow across cell membranes (transcellular) or along cytoplasmic continuities formed by plasmodesmata (symplastic) [1]. Extracellular hydrophobic barriers of lignin and suberin located in the endodermis are thought to restrict diffusion of water along the apoplastic path [2]. In the presence of such barriers, water channels present in cell membranes called aquaporins enable cell to cell transport [3].

Aquaporins (AQP) are present across life forms, with the exception of thermophilic Archaea and intracellular bacteria [4]. They belong to the Major Intrinsic Proteins (MIP) superfamily and are characterized by six transmembrane domains and two highly conserved Asn-Pro-Ala (NPA) motifs [5]. Another typical AQP signature is selectivity filters structuring the pore, which are composed of aromatic/arginine (ar/R) motifs and Froger's residues [6, 7]. In higher plants, AQP isoforms fall into five families; Plasma membrane Intrinsic Proteins (PIP), Tonoplast Intrinsic Proteins (TIP), Nodulin26-like Intrinsic Proteins (NIP), Small Intrinsic Proteins (SIP) and uncharacterized (X) Intrinsic Proteins (XIP) [8]. Although plant AQP are localized throughout the cell secretory system, PIP, NIP and XIP are preferentially located in plasma membranes, while TIP accumulate in the tonoplast and SIP in the endoplasmic reticulum [9–11]. Functional studies, combined with modelling approaches demonstrated that in addition to being permeable to water, AQP also transport other substrates [12, 13]. Some PIP isoforms are permeable to hydrogen peroxide (H_2O_2), nitrate (NO_3^-) and carbon dioxide (CO_2), some TIP isoforms to ammonia (NH_3) and urea, and some NIP to small organic solutes or mineral nutrients [14–19]. AQP possess wide range of physiological functions and have now been identified in a number of crop species such as rice, maize, tomato, cotton, sorghum, foxtail millet, watermelon and cannabis [20–25].

In plants, AQP are involved in water transport in both roots and shoots. In Arabidopsis, isoforms AtPIP2-2 and AtPIP1-2 contribute around 14% and 20% of the root osmotic conductivity and shoot hydraulic conductivity, respectively [26, 27]. AQP also have important roles in plant growth, CO_2 fixation, nutrient allocation, reproduction or biotic interactions [8]. In recent years, AQP functions in plant water relations have received more attention as a potential target for crop improvement [28–33]. For instance, AQP could contribute to balancing root water transport with transpiration in soybean under high evaporative demand [34]. This hypothesis is supported by the increased AQP expression and root hydraulic conductivity upon high transpiration demand in rice and grapevine [35, 36]. Furthermore, overexpression of *SiTIP2-2* in tomato increased transpiration rate and was associated with improved fruit yield upon moderate soil water stress [37]. Conversely, in other crops more adapted to hot and dry climates such as pearl millet, lower transpiration under high vapor pressure deficit (VPD) has been associated with AQP function and proposed to be beneficial for crop yield under such conditions [31, 38, 39]. Therefore, AQP may be involved in different physiological mechanisms that determine the rate and pattern of plant water usage [40]. In fact, specific isoforms might be involved in different scenarios, calling for a better understanding of AQP family members and their functions in crops [29].

Pearl millet [*Pennisetum glaucum* (L) R Br.] is a key cereal for food security in arid and semi-arid regions [41]. However, its yields are low and are often affected by climate unpredictability (heat waves and dry spells), which is forecast to worsen [42, 43]. The recent release of the pearl millet genome has opened new opportunities for functional genomic-based efforts to improve pearl millet yield and abiotic stress tolerance [44]. In this study, links between AQP function in roots and water use were investigated by measuring AQP contribution to Lpr in two pearl millet inbred lines contrasting for water use efficiency. The entire AQP family in pearl millet was characterized using a genomic approach and analyses of root AQP gene expression provided insights into how AQP isoform contribute to root hydraulics.

Materials and methods

Plant material and growth conditions

IP4952 and IP17150, two pearl millet inbred lines that are part of the Pearl Millet inbred Germplasm Association Panel (PMiGAP) were used in this study [44]. The water use efficiency (expressed as a plant biomass produced per amount of water transpired in $g.kg^{-1}$) of these two lines was characterized in two lysimeters experiments performed under well-irrigated conditions at the International Crops Research Institute for the Semi-Arid Tropics (ICRISAT, India) using the protocol outlined in [45]. These experiments indicated that IP4952 and IP17150 displayed relatively low and high water use efficiency, respectively (2.35 versus 3.72 $g.kg^{-1}$) [46]. These two lines were used for root hydraulic conductivity measurements and AQP expression analyses in which plants were grown in hydroponic conditions in a nethouse (greenhouse made of shade nets) at the IRD/ISRA Bel Air research station (Dakar, Senegal; 14.701615 N– 17.425359 W). Plants were germinated in Petri dishes in a dark chamber at 37˚C for two days. Plants were exposed to light (37˚C, 12h day/night cycle) for one day before being transplanted to a black mat covering a 30L container (45x40x24 cm containing 40 plants in total) filled with half strength Hoagland solution [47]. The system allowed roots to grow in the nutrient solution without been exposed to light. Oxygen was constantly supplied to the root zone using an air pump.

Root hydraulic conductivity and aquaporin contribution

Root hydraulic conductivity (Lpr) was measured in April-May 2019 from 9AM to 12PM on 15 day old plants. Minimum and maximum temperature and humidity over the period of plant growth was 17/34˚C and 34/100%. At the time of measurements, average temperature, relative humidity and VDP were 24.4 ± 0.3˚C, 75.1 ± 1.2% and 0.8 ± 0.1, respectively. Plants replicates were grown sequentially to allow analysis at the same age, in a randomized design taking into account the time of measurement. Lpr measurements were performed using a pressure bomb (model 1000, PMS instrument company, USA) according to [48] and [49]. Briefly, plants were inserted into the pressure chamber filled with nutrient solution with our without 2mM azide (NaN_3). The hypocotyl was carefully threated through the silicone grommet of the pressure chamber lid so the intact root system was sealed into the chamber. Roots were pressurized with compressed air at 0.4 MPa for 5 min to equilibrate, followed by xylem sap collection at 0.1, 0.2 and 0.3 MPa for 5 min using pre-weighed 2 ml Eppendorf tubes filled with cotton placed on top of the stem. The mass of xylem sap exuded at each pressure was determined by weighing and was used to calculate root conductance (L_0; slope of xylem sap weight at each pressure). After the measurements, roots systems were scanned to determine average root diameter, length and root surface area using WinRhizo Pro version 2012b (Regent Instruments, Canada). Root conductance was divided by root surface area to calculate Lpr. AQP contribution to Lpr was estimated using relative Lpr inhibition by azide calculated as:

$$100 - ((\mathrm{Lpr}_{\mathrm{azide\_individual\_replicate}} \times 100)/\mathrm{Lpr}_{\mathrm{no\_azide\_variety\_mean}}) \quad (1)$$

Genome-wide aquaporin identification

A total of 772 AQP protein sequences from 19 plant species (*Arabidopsis thaliana*, *Beta vulgaris*, *Brachypodium distachyon*, *Cicer arietinum*, *Gossypium hirsutum*, *Glycine max*, *Hordeum vulgare*, *Linum usitatissimum*, *Musa acuminate*, *Panicum virgatum*, *Pennisetum glaucum*, *Populus tremula*, *Oryza sativa*, *Setaria italica*, *Solanum lycopersicum*, *Solanum tuberosum*, *Sorghum bicolor*, *Vitis vinifera* and *Zea mays*) were aligned against the pearl millet genome (ASM217483v2) and the non-assembled pearl millet scaffolds [44] using tblastn with an e-

value of 10^{-5} as initial cut-off to identify high scoring pairs. High scoring pairs were further filtered to keep those with a bit score $\geq$100. Hot-spots of high scoring pairs were identified and redundant high scoring pairs were filtered to keep those with highest bit-score for further analysis (S1 Table). The locations of filtered high scoring pairs in the pearl millet genome were used to identify regions with homologies to AQP genes.

Structural annotation

Correspondence between selected high scoring pairs and annotated genes in the pearl millet genome was investigated. Potential AQP genes were identified and their genomic sequence ± 1000pb upstream and downstream of the start/end position was retrieved as well as the predicted gene structure [44]. When predicted high scoring pairs did not correspond to previously annotated genes, the GENSCAN Web Server (http://hollywood.mit.edu/GENSCAN.html) was used to predict the exon-intron structure of the genomic region. Putative AQP genomic sequences were aligned against the Plant EST (downloaded in August 2018) and the UniProt/Swiss-Prot plant protein (February 2016) databases and were manually annotated using the Artemis software (version 17.0.1, Sanger Institute, UK; S2 Table). Annotation was confirmed by aligning reads from pearl millet transcriptomes [50] against the pearl millet genome using the Tablet software (version 1.19.09.03) [51]. Coding and protein sequences were then generated. AQP gene structure were visualized using GSDS2.0 software [52]. The genomic, coding and protein sequences of the pearl millet AQP genes are available at the following address: https://dataverse.ird.fr/dataset.xhtml?persistentId=doi:10.23708/WVCG5O.

Sequencing

AQP genes with incomplete sequences in coding regions were resequenced (S2 Table) using genomic DNA or cDNA from Tift 23D2B1 (genotype used to draft the pearl millet whole genome sequence). DNA was prepared using DNeasy Plant mini extraction kit (Qiagen, Germany). cDNA was prepared by first extracting RNA using the RNeasy Plant mini extraction kit (Qiagen, Germany), followed by DNAse treatment (RNase-free DNase set; Qiagen, Germany) and then reverse transcription reaction (Omniscript RT kit; Qiagen, Germany), according to the manufacturer's instructions. Corresponding DNA/cDNA fragments were amplified using the Phusion high-fidelity DNA polymerase (Thermo Scientific, USA), purified (Geneclean turbo kit, MP Biomedicals, USA) and sent for sequencing (Eurofins Genomics, Germany). These new sequences are referenced in Genbank under the accession number MT474859 for *Pennisetum glaucum* (Pg) PIP2-8, MT474860 for PgTIP3-1, MT474861 for PgTIP4-1, MT474862 for PgTIP4-2, MT474863 for PgTIP4-3, MT474866 for PgNIP1-2, MT474867 for PgNIP3-5, MT474868 for PgSIP1-2 and MT474869 for PgSIP2-1. Primers used for amplification are presented in S3 Table. Difficulties in amplifying the missing sequence of PgTIP5-1 were encountered. In that specific case, unpublished MINION reads (Mariac, Vigouroux, Berthouly-Salazar; unpublished) were used to complete its sequence (Genbank accessions MT474864 and MT474865). Missing nucleotides were assembled onto the pearl millet genomic sequence and the coding frame of the new protein was determined.

Identification of functional motifs and transmembrane domains

The NCBI conserved domain database (CDD) was used to identify Asn-Pro-Ala (NPA) motifs and aromatic/arginine (ar/R) selectivity filters in the putative AQP protein sequences. Froger's residues were identified according to [6]. The number and location of the transmembrane domains were studied using TMHMM (http://www.cbs.dtu.dk/services/TMHMM/), TMpred (https://embnet.vital-it.ch/software/TMPRED_form.html) and Phyre2 [53]. Protein sequences

were aligned using the CLUSTALW alignment function in the Maga7 software (version 7.0.26) [54]. Alignments were colored using the Color Align Properties program (https://www.bioinformatics.org/sms2/color_align_prop.html). Conserved domains, as well as transmembrane domains, were further manually analyzed to detect sequence alterations. Phyre2 was also used to predict *Pennisetum glaucum* PIP (PgPIPs) structure based on homologies with aquaporins of known structure. This generated Protein Data Bank (PDB) files that were used for studying three-dimensional geometric structure and pore morphology of PIP using PoreWalker software (https://www.ebi.ac.uk/thornton-srv/software/PoreWalker/). The PDB files are available at the following address: https://dataverse.ird.fr/dataset.xhtml?persistentId=doi:10.23708/WVCG5O.

Phylogenetic analysis

Phylogenetic analyses of *P. glaucum* AQP (PgAQP) was conducted including AQP identified in *A. thaliana* (AtAQP), *O. sativa* (OsAQP) and *P. tremula* (PtAQP) using the Mega7 software (version 7.0.26) [54]. PgAQP, AtAQP, OsAQP and PtAQP protein sequences were aligned using the CLUSTAW function and a phylogenetic tree was built using the maximum likelihood method with 1000 reiterations. This allowed determination of the statistical stability of each node. Based on their position in the phylogenetic tree, PgAQP isoforms were classified into PIP, SIP, TIP and NIP families and named according to their close homologs.

Expression profiling

Quantitative polymerase chain reaction (RT-PCR) was used to measure PgPIP gene expression in 15 day old plants grown in hydroponic conditions. One seminal and one crown root were collected between 10AM and 12PM. Sampled roots were immediately frozen using liquid nitrogen and later ground using a TissueLyser II (Qiagen). RNA and cDNA (from 1μg of RNA) were prepared using extraction kits as described above. RT-PCR was performed with 1μL of diluted cDNA (1:9) in a Brillant III ultra fast SYBRgreen QPCR master mix (Agilent Technologies, USA) using a StepOnePlus Real-Time PCR System (Applied biosystems, USA). Primers used to amplify the different PgPIP genes were checked for specificity and efficiency prior to the experiment (S4 Table). The pearl millet Ubiquitin gene (*Pgl_GLEAN_10001684*) was used as a reference and PgPIP relative expression was calculated according to the delta-delta ct method.

Data to characterize PgAQP shoot expression profiles were collected from [50]. Leaves and inflorescence of ten open pollinated cultivated pearl millet varieties were used [50].

Statistics

Statistical analyses were performed using R version 3.5.2 (R Development Core Team, 2018) using ANOVA (aov script) to detect significant differences. The Least Significant Difference (LSD) test, within the Agricolae package, was used to group differences in letter classes.

Results

Pearl millet aquaporin contribution to root hydraulic conductivity

In order to determine if AQP function and root radial water flow could be associated with water use in pearl millet, we measured root hydraulic conductivity (Lpr) in IP4952 and IP17150, previously described as low and high water use efficiency lines, respectively. These lines did not show significant differences in root diameter and root surface area at the time of Lpr measurement, although root length was significantly higher in IP17150 as compared to

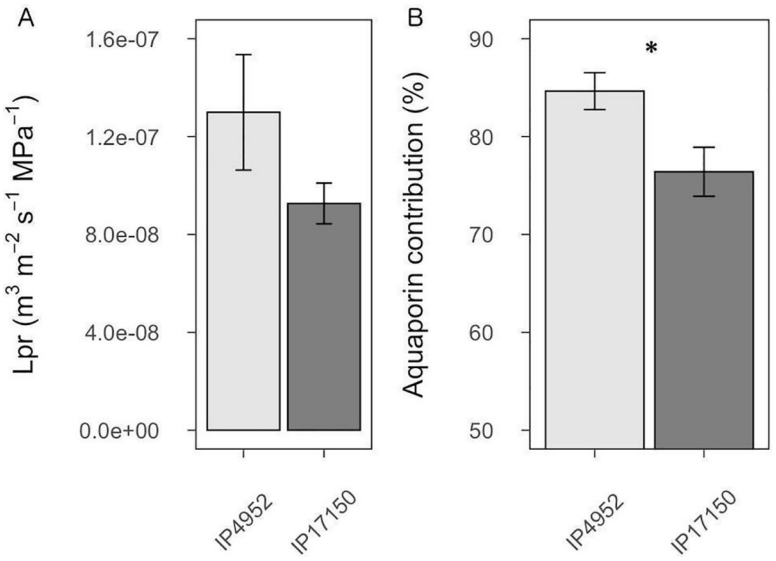

Fig 1. Root hydraulic conductivity and aquaporin contribution in roots of IP4952 and IP17150. Root hydraulic conductivity (Lpr) was measured in plants grown in hydroponic conditions between 9AM to 12PM with or without 2mM azide. (A) Lpr values were measured without azide. (B) Aquaporin contribution to Lpr shown as relative difference between Lpr of azide treated and non-azide treated plants. Bars represent mean values ± se of n = 10–15 plants. *: $p < 0.05$.

https://doi.org/10.1371/journal.pone.0233481.g001

IP4952 ($p < 0.05$; S5 Table). No significant differences in L_0 and Lpr ($p = 0.148$) were observed between IP4952 and IP17150 (Fig 1 and S6 Table). In both IP4952 and IP17150, treatment with azide, an inhibitor of AQP activity, led to significant L_0 and Lpr reduction ($p < 0.001$; S6 Table). Significant differences in L_0 were observed between lines in the presence of azide (S6 Table), indicating genotypic differences in anatomical traits. This effect of azide application on Lpr was mostly reversible after treating the same roots with azide-free solution (S1 Fig). AQP contribution to Lpr was significantly higher in IP4952 (low water use efficiency) as compared to IP17150 (high water use efficiency; 84.64 ± 1.98% versus 76.40 ± 2.61%, $p < 0.05$; S6 Table). Therefore, Lpr inhibition by azide indicates that AQP could contribute more than 75% to Lpr in pearl millet.

Aquaporin identification and annotation

To gain insight on the AQP isoforms contributing to Lpr in pearl millet, we characterized AQP gene families in the pearl millet genome. We blasted 772 AQP protein sequences identified in 19 different species on the pearl millet reference genome (chromosome assembly and scaffolds) [44]. A total of 7005 sequences with bit score >100, representing 50 specific hits were identified (S1 Table). Forty-seven of the hits fell within previously annotated genes, one fell in a non-annotated part of the genome on chromosome 5, and two in non-assembled parts of the genome (scaffold763 and scaffold8428).

Manual *de novo* annotation of the 50 putative AQP genes allowed the identification of eight genes with no start or with early stop codons in the first exon that were classified as pseudogenes (S2 Table). Nine genes did not encode AQP isoforms but rather zinc-finger protein/LRR receptor-like serine-threonine protein kinase families or DEAD-like helicase-N protein superfamilies. The absence of AQP signature domains (NPA and Ar/R motifs) in their protein sequence confirmed their non-affiliation to the AQP family. A number of genes showed an excessive number of exons or longer first exon and were re-annotated on the basis of

alignment with transcriptome sequences or with close protein homologs (Uniprot/Swiss-Prot blast results) and presence of AQP isoform conserved domains. In addition, ten genes showing missing sequences in coding regions were newly assembled and annotated after sequencing. Overall, 33 *Pennisetum glaucum* AQP (PgAQP) genes were identified in the pearl millet genome, sixteen of which were annotated *de novo* (Table 1).

Table 1. Description and distribution of pearl millet aquaporin genes.

ID	Gene	Pgl_Glean ID	Gene length (bp)	Transcript length (bp)	Protein length (aa)	Protein MW (kD)	Chr	Start	End
Plasma membrane intrinsic proteins (PIP)									
1	*PgPIP1-1*	*Pgl_GLEAN_10001520*	3097	867	288	30.70	3	5721622	5724718
2	*PgPIP1-3*	*Pgl_GLEAN_10010809*	1601	867	288	30.76	3	274573998	274575598
3	*PgPIP1-4*	*Pgl_GLEAN_10005724*	992	900	298	31.38	2	104247932	104248932
4	*PgPIP2-1*	*Pgl_GLEAN_10028064*	2920	873	290	30.35	3	12453415	12456334
5	*PgPIP2-2*	*Pgl_GLEAN_10028876*	2830	867	288	30.12	3	45603209	45606038
6	*PgPIP2-3*	*Pgl_GLEAN_10035675*	1903	873	290	30.39	3	257669631	257671533
7	*PgPIP2-5*	*Pgl_GLEAN_10028056*	1062	834	277	28.93	3	12167791	12168852
8	*PgPIP2-6*	*Pgl_GLEAN_10028055*	1053	861	286	29.94	3	12156953	12158005
9	*PgPIP2-7*	*Pgl_GLEAN_10010255*	1170	861	286	29.79	Scaffold763	240584	241753
10	*PgPIP2-8*	*Pgl_GLEAN_10009812*	837	837	278	29.17	2	64966663	64967453
Tonoplast intrinsic proteins (TIP)									
11	*PgTIP1-1*	*Pgl_GLEAN_10002147*	1499	750	249	25.72	5	153303973	153305471
13	*PgTIP2-1*	*Pgl_GLEAN_10000631*	844	744	247	24.88	2	30657555	30658398
16	*PgTIP2-2*	*Pgl_GLEAN_10030617*	933	747	248	25.03	3	100540239	100541171
12	*PgTIP2-3*	*Pgl_GLEAN_10009584*	851	750	249	25.06	3	33622445	33623295
15	*PgTIP3-1*	*Pgl_GLEAN_10028702*	911	801	266	27.41	2	44624536	44625481
14	*PgTIP4-1*	*Pgl_GLEAN_10002901*	2557	738	245	25.58	1	263875434	263878070
18	*PgTIP4-2*	*Pgl_GLEAN_10003219*	1455	744	247	25.15	3	148813464	148814777
17	*PgTIP4-3*	*Pgl_GLEAN_10003218*	844	747	248	25.10	3	148807632	148808412
19	*PgTIP5-1*	*Pgl_GLEAN_10033583*	1087	813	270	26.69	3	272599938	272601028
Noduline-26 like intrinsic proteins (NIP)									
20	*PgNIP1-1*	*Pgl_GLEAN_10012175*	2316	846	281	29.52	2	195368171	195370486
21	*PgNIP1-2*	*Pgl_GLEAN_10028618*	2560	846	281	29.53	1	261387113	261389753
22	*PgNIP1-4*	*Pgl_GLEAN_10028339*	1137	837	278	29.36	3	145385690	145386826
23	*PgNIP2-1*	*Pgl_GLEAN_10018521*	3364	891	296	31.82	3	14105646	14109009
24	*PgNIP2-2*	*Pgl_GLEAN_10019286*	3821	894	297	31.57	2	103033018	103036838
25	*PgNIP3-1*	*Pgl_GLEAN_10034621*	3855	909	302	31.43	2	40497062	40500916
26	*PgNIP3-2*	*Pgl_GLEAN_10030882*	1151	846	281	29.60	4	55609410	55610656
27	*PgNIP3-3*	*Pgl_GLEAN_10030883*	1087	780	259	27.05	4	55648949	55650374
28	*PgNIP3-4*	*Pgl_GLEAN_10030881*	1258	750	249	25.15	4	55573901	55575272
29	*PgNIP3-5*	*Pgl_GLEAN_10030872*	934	837	278	27.79	4	55508562	55509419
30	*PgNIP4-1*	*Pgl_GLEAN_10012100*	1319	921	306	31.52	6	110090448	110091766
Small intrinsic proteins (SIP)									
31	*PgSIP1-1*	*Pgl_GLEAN_10003744*	2818	726	241	25.32	1	175152169	175154986
32	*PgSIP1-2*	*Pgl_GLEAN_10014008*	3375	759	252	25.91	4	93394125	93397493
33	*PgSIP2-1*	*Pgl_GLEAN_10026167*	1899	759	252	27.10	5	126489209	126491163

PgPIP2-7 is located on scaffold763, which was not assembled to the pearl millet genome. bp: base pairs; aa: amino-acids; MW: molecular weight; kD: kilo Dalton; Chr: chromosome; Start: position of the ATG; End: position of the stop codon.

https://doi.org/10.1371/journal.pone.0233481.t001

Pearl millet aquaporins phylogenic analysis

To classify the PgAQP into families and name them, a phylogenetic tree was built using the PgAQP protein sequences along with protein sequences from *Arabidopsis thaliana*, *Oryza sativa* and *Populus tremula* (Fig 2). The PgAQP were named according to their grouping into families (PIP, TIP, SIP or NIP) and close homologs (Table 1). Ten isoforms showed homologies to the PIP family with three isoforms falling in the PIP1 sub-family (PgPIP1-1, PgPIP1-3 and PgPIP1-4) and seven isoforms falling in the PIP2 sub-family (PgPIP2-1, PgPIP2-2, PgPIP2-3, PgPIP2-5, PgPIP2-6, PgPIP2-7 and PIP2-8). Nine isoforms from the *P. glaucum* TIP family (PgTIP), eleven isoforms from the *P. glaucum* NIP family (PgNIP) and three isoforms from the *P. glaucum* SIP family (PgSIP) were further identified. No isoforms from the XIP family were identified in pearl millet. This analysis further confirmed the classification of PgPIP1-1, PgPIP2-1, PgPIP2-3, PgPIP2-6, PgTIP1-1 and PgTIP2-2 cloned by [31]. However, PgPIP1-2 from [31] was renamed as PgPIP1-3 in this study.

Most PgAQP genes were localized on chromosome 3 and none were localized on chromosome 7 (Fig 3). Two PgAQP hot-spots were observed, one in a region of 11899bp on chromosome 3 containing *PgPIP2-1*, *PgPIP2-5* and *PgPIP2-6* and the other in a region of 141812bp on chromosome 4 containing *PgNIP3-2*, *PgNIP3-3*, *PgNIP3-4* and *PgNIP3-5*.

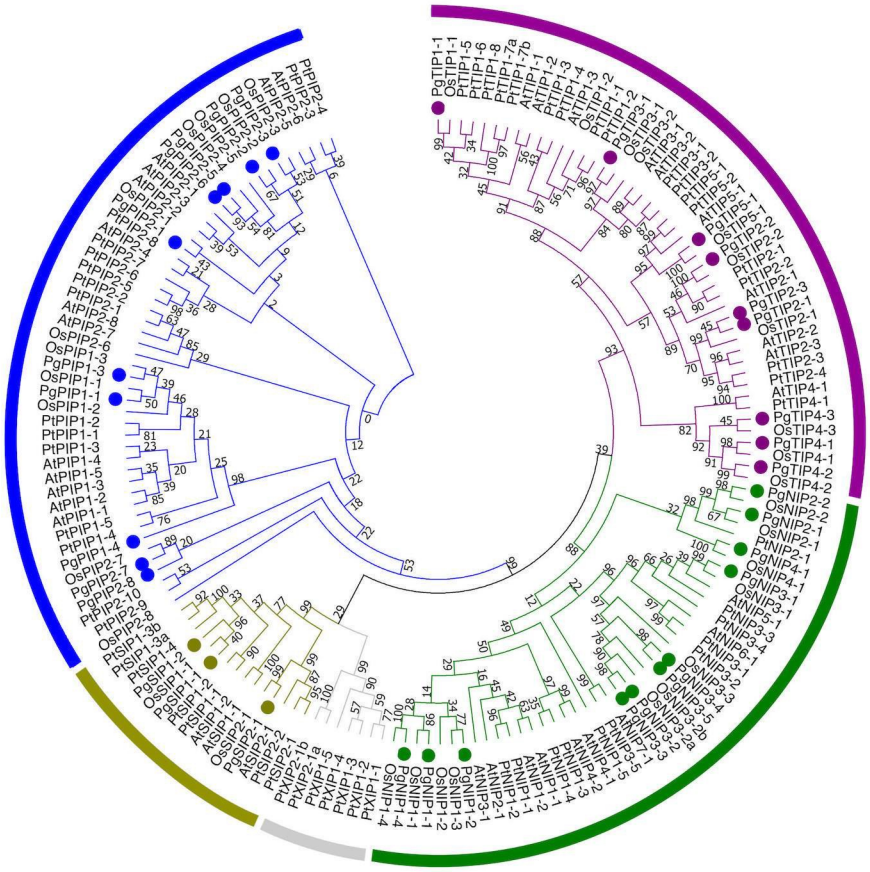

Fig 2. Phylogenetic relationship among aquaporins isoforms from pearl millet, Arabidopsis, rice and poplar. A phylogenetic tree was generated using the Maximum Likelihood method with 1000 reiterations in MEGA7. Bootstrap values above 50% are represented. The PIP, TIP, SIP, NIP and XIP family clades are represented by blue, grey, purple, green and red, respectively. Pearl millet sequences are indicated by colored dots.

https://doi.org/10.1371/journal.pone.0233481.g002

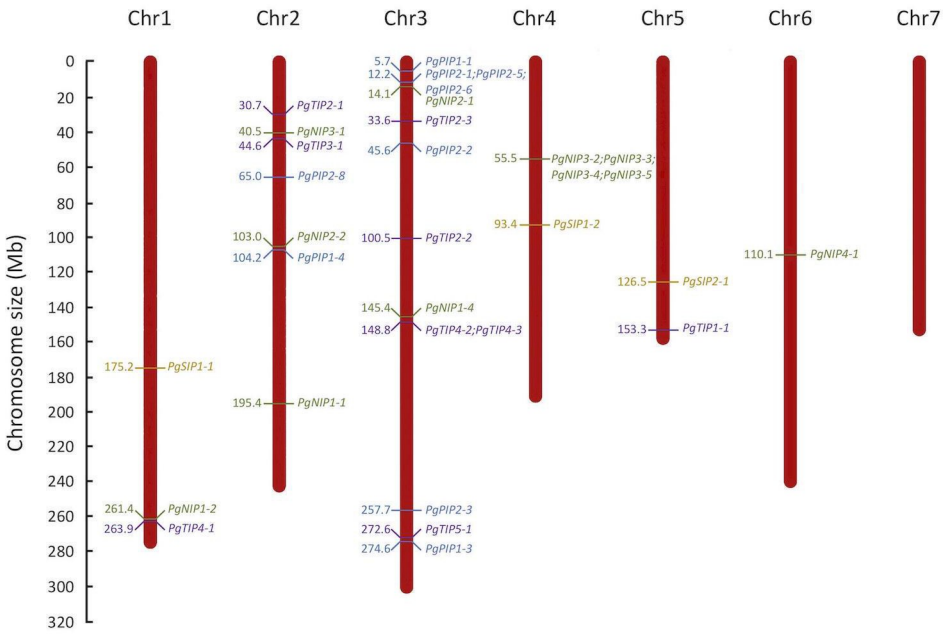

Fig 3. Distribution of aquaporin genes in the pearl millet genome. The seven chromosomes (Chr) of the pearl millet genome are represented according to their size in megabase (Mb). Positions of PIP, TIP, SIP and NIP genes are represented in blue, purple, orange and green, respectively. *PgPIP2-7*, which is localized on scaffold763, is not represented.

https://doi.org/10.1371/journal.pone.0233481.g003

Aquaporin gene structure in pearl millet

PgAQP genes showed large variation in gene length (ranging from 837bp for *PgPIP2-8* to 3855bp for *PgNIP3;1*; Table 1). Transcript lengths were less variable and relatively conserved within families, with lengths of around 800-900bp for the PgPIP and PgNIP genes, 750-800bp for the PgTIP genes and 700-750bp for the PgSIP genes.

To further confirm the phylogenetic classification, gene structure of the PgAQP genes was analyzed (S2 Fig). PgAQP genes displayed between one (*PgPIP2-8*) and five exons (*PgNIP2-1*, *PgNIP2-2* and *PgNIP4-1*). Except for the NIP family, intron-exon organization was generally conserved within families with 5 of 9 PgPIP genes displaying 3 exons, 6 of 9 PgTIP genes displaying 2 exons and all PgSIP genes displaying 3 exons, supporting their phylogenetic distribution. Furthermore, *PgPIP2-5*/*PgPIP2-6* and *PgNIP3-2*/*PgNIP3-3* were found to be close homologs in the phylogenetic analysis (Fig 2), and were located near each other on the pearl millet genome (Fig 3). They showed similar gene and transcript length (Table 1) as well as gene structure (S2 Fig).

PgAQP coding regions encoded proteins with length varying between 250 to 300 amino acids, with molecular weight of around 30kD for the PgPIP and PgNIP and 25kD for the PgTIP and PgSIP isoforms (Table 1).

Pearl millet AQP conserved domains

Analysis of selectivity filters and transmembrane domains was performed to investigate polymorphisms that could impact substrate selectivity of the PgAQP. Analysis of conserved domains showed that all PgAQP isoforms belonged to the MIP super-family and displayed typical double NPA motifs (S7 Table and Table 2). Although some polymorphisms in NPA motifs were observed in some isoforms (particularly from the NIP family), subsequent amino-acids had the same chemical properties (generally neutral and non-polar; Table 2, Fig 4 *and*

Table 2. Amino-acids residues in conserved domains of pearl millet aquaporins isoforms.

Isoform	NPA (LB)	NPA (LE)	Ar/R selectivity filters				Froger's residue				
			H2	H5	LE1	LE2	P1	P2	P3	P4	P5
Plasma membrane intrinsic proteins (PIP)											
PgPIP1-1	NPA	NPA	F	H	T	R	Q	S	A	F	W
PgPIP1-3	NPA	NPA	F	H	T	R	Q	S	A	F	W
PgPIP1-4	NPA	NPA	F	H	T	R	V	S	A	F	W
PgPIP2-1	NPA	NPA	F	H	T	R	Q	S	A	F	W
PgPIP2-2	NPA	NPA	F	H	T	R	Q	S	A	F	W
PgPIP2-3	NPA	NPA	F	H	T	R	Q	S	A	F	W
PgPIP2-5	NPA	NPA	F	H	T	R	-	S	A	F	W
PgPIP2-6	NPA	NPA	F	H	T	R	Q	S	A	F	W
PgPIP2-7	NPA	NPA	F	H	T	R	T	S	A	F	W
PgPIP2-8	NPA	NPA	F	H	T	R	H	S	A	F	W
Tonoplast intrinsic proteins (TIP)											
PgTIP1-1	NPA	NPA	H	I	A	V	T	S	A	Y	W
PgTIP2-1	NPA	TPA	H	I	G	R	T	S	A	Y	W
PgTIP2-2	NPA	NPA	H	I	G	R	T	S	A	Y	W
PgTIP2-3	NPA	NPA	H	I	G	R	T	S	A	Y	W
PgTIP3-1	NPA	NPA	H	V	A	R	T	V	A	Y	W
PgTIP4-1	NPS	NPA	N	S	A	R	T	S	A	Y	W
PgTIP4-2	NPA	NPA	Q	S	A	R	T	S	A	Y	W
PgTIP4-3	NPA	NPA	H	I	A	H	T	S	A	Y	W
PgTIP5-1	NPA	NPA	Q	V	A	R	R	S	A	Y	W
Noduline-26 like intrinsic proteins (NIP)											
PgNIP1-1	NPA	NPA	W	V	A	R	F	T	A	Y	V
PgNIP1-2	NPA	NPA	W	V	A	R	F	T	A	Y	F
PgNIP1-4	NPA	NPV	W	A	A	R	F	S	A	Y	I
PgNIP2-1	NPA	NPA	G	S	G	R	L	T	A	Y	F
PgNIP2-2	NPA	NPA	G	S	G	R	L	T	A	Y	F
PgNIP3-1	NPS	NPV	A	I	G	R	F	T	A	Y	L
PgNIP3-2	NPA	NPA	A	A	A	R	Y	T	A	Y	M
PgNIP3-3	NPA	NPA	A	A	A	R	Y	T	A	Y	M
PgNIP3-4	NPA	NPA	A	A	A	R	Y	T	A	Y	M
PgNIP3-5	NPA	NPA	A	A	A	R	Y	T	A	Y	M
PgNIP4-1	NPA	NPI	M	G	G	R	M	T	A	Y	L
Small intrinsic proteins (SIP)											
PgSIP1-1	NPT	NPA	V	V	P	N	M	A	A	Y	W
PgSIP1-2	NPT	NPA	L	I	P	N	M	A	A	Y	W
PgSIP2-1	NPL	NPA	S	H	G	S	F	A	A	Y	W

The two NPA (Asparagine-Proline-Alanine) motifs are located on loop B (LB) and loop E (LE). Aromatic/Arginine motifs (Ar/R) are located on helix 2 (H2), helix 5 (H5), and loop E (LE1 and LE2). P1-5 designed the five Froger's position.

https://doi.org/10.1371/journal.pone.0233481.t002

S3–S5 Figs). Ar/R selectivity filters and Froger's residues were well conserved in the PgPIP isoforms, except for the Froger's residue on position 1 (P1; Table 2, Fig 4). More polymorphisms were observed in these residues for the PgTIP, PgNIP and PgSIP isoforms although the ar/R residue on Loop E (R on LE2) and the Froger's residues at positions 3 (A) and 4 (F/Y) were well conserved across all isoforms (Table 2).

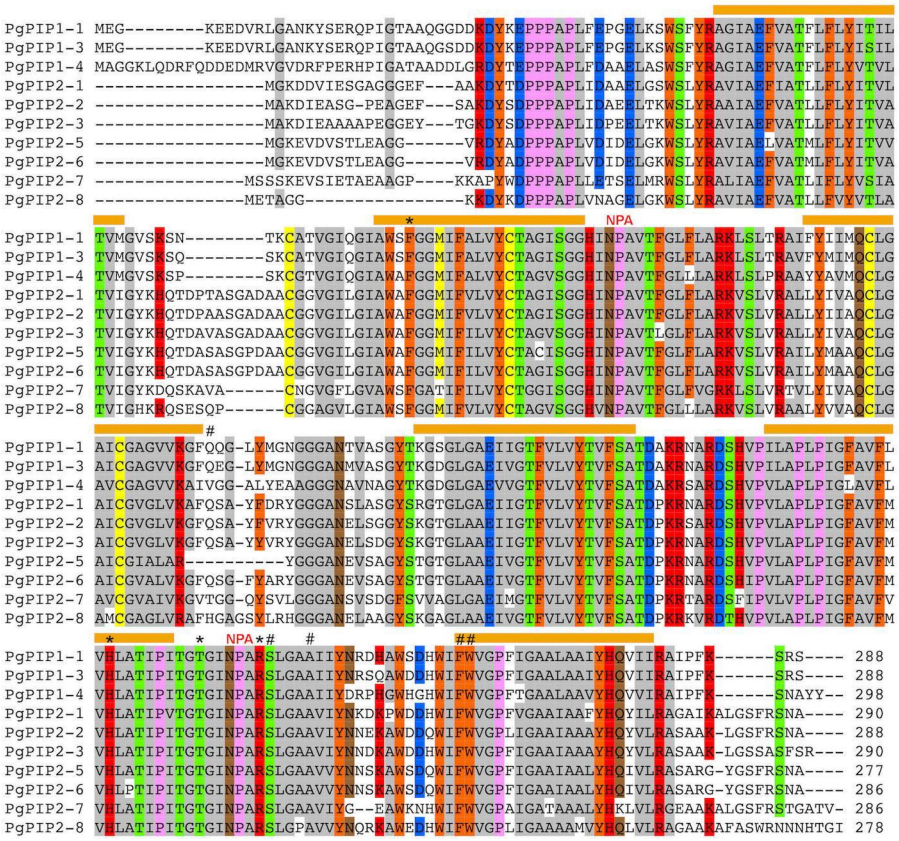

Fig 4. Conserved domains and membrane topology of the PIP isoforms from pearl millet. Alignment of the PIP isoforms were obtained using ClustalW in Mega7. Sequence identities and similarities (80%) are highlighted in colors. The transmembrane domains are represented by orange bars with the N-terminal and C-terminal ends of the protein located in the cytosol. NPA: Asparagine-Proline-Alanine motifs; *: Aromatic/Arginine selectivity filters. #: Froger's residues.

https://doi.org/10.1371/journal.pone.0233481.g004

Transmembrane domain analyses using three different types of prediction software suggested a high probability that all identified PgAQP possess six transmembrane domains with cytoplasmic N-terminal and C-terminal ends, as is typically observed for AQP (S8 Table). Predictions of 3-dimensional geometric structure and pore morphology suggested a continuous pore that runs longitudinally across both sides of the membranes for all PgPIP (S6 Fig). Two constrictions in the pore center were typically observed at both extremities, illustrating the two constraints caused by the NPA motifs.

Aquaporin expression profiling in pearl millet

PIP isoforms are thought to play major roles in root hydraulic conductivity because of their localization at the plasma membrane [8]. To infer PgPIP isoforms putative importance to Lpr in pearl millet, we analyzed PgPIP gene expression pattern in roots of IP4952 and IP17150 using quantitative PCR. PgPIP genes were generally more expressed in IP4952 as compared to IP17150 (Fig 5). In both lines, *PgPIP1-1*, *PgPIP1-3*, *PgPIP1-4*, and *PgPIP2-3* were most expressed while *PgPIP2-5*, *PgPIP2-6*, *PgPIP2-7* and *PgPIP2-8* were less expressed. *PgPIP1-3* and *PgPIP1-4* were the only genes significantly differently expressed between both lines.

Expression of PgPIP in shoots (leaves and inflorescence) were retrieved from [50]. Transcriptomic analyses from ten pearl millet varieties suggest that *PgPIP1-4* and *PgPIP2-3*, two of

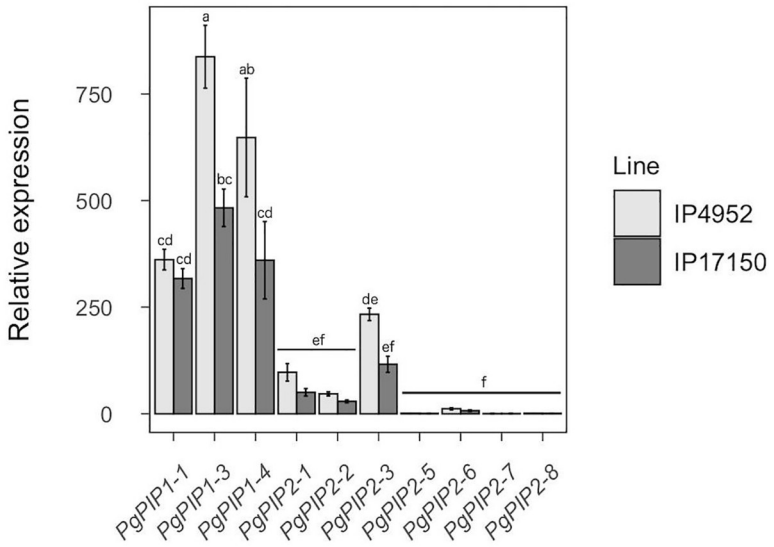

Fig 5. Relative expression of PIP genes in roots of IP4952 and IP17150. Transcript abundance of each PIP genes were measured between 9AM and 12PM on plants grown in hydroponic conditions and normalized to the expression of *PgPIP2-5* in IP4952. Bars show mean values ± se of n = 6–8 biological replicates, each with three technical replicates. Letters indicate significance difference among groups.

https://doi.org/10.1371/journal.pone.0233481.g005

the most expressed genes in roots, are expressed at low levels in shoots (S7 Fig). Conversely, *PgPIP1-1* and *PgPIP1-3* are highly expressed in roots and shoots.

Discussion

Investigation of the role of AQP in root water transport in pearl millet, a heat and drought-adapted crop, suggest that PgAQP are major contributors to root water flow. Root hydraulic conductivity (Lpr) varied around 1E-07 m^3 m^{-2} s^{-1} MPa^{-1}, within the previously report range of other plants [55]. Treatment of roots with a common AQP inhibitor (azide) suggested that AQP contribute up to 84% of Lpr in pearl millet (S6 Table). This figure is higher than what has been observed in Arabidopsis (57 to 64%) [56] and rice (42 to 79%) [57]. However, complete Lpr recovery following inhibition by azide (S1 Fig) suggests AQP contribution was not over-estimated due to off-target effects of azide.

The AQP gene family of the pearl millet genome was characterized and thirty-three putatively functional AQP isoforms (based on conserved domains and protein topology) were identified, belonging to the PIP (10), TIP (9), SIP (3) and NIP (11) families. No XIP were identified, which confirm the absence of isoforms from this family in the monocotyledon clade [8]. The number of AQP identified in pearl millet is similar to what has been observed in Arabidopsis (35) [58], rice (33) [23] and maize (31) [20]. Interestingly, AQP genes were over-represented on Chromosome 3 with fourteen genes (Fig 3). The proximal localization of *PgPIP2-5* and *PgPIP2-6* in Chromosome 3, their phylogenetical relatedness and similar gene structure (Fig 3 and S2 Fig), suggest possible tandem duplication events in this region [59]. Similarly, *PgNIP3-2* and *PgNIP3-3*, located on Chromosome 4 may be the result of duplication events. Furthermore, *PgPIP2-7* was identified in scaffold763 suggesting that genes may be missing on parts of the pearl millet genome assembly.

The selectivity of an AQP is defined by the three dimensional structure of the amino-acids constituting its pore. The NPA motifs on loops B and E contribute to the dipole moment of the α-helices and prevent proton permeation [60, 61]. These motifs were strictly conserved in

PgPIP but showed some polymorphisms for other isoforms (Table 2). However, these substitutions did not drastically change the positive electrostatic potential at the NPA motifs, suggesting that proton exclusion from AQP pores is conserved in pearl millet. Furthermore, the Isoleucine (I) preceding the Froger's residue P4 and P5 at the end of Loop E, shown to be essential for CO_2 transport in PIP [62], is conserved in PgPIP (Fig 4).

The ar/R motifs, composed of four amino-acids, restrict extracytosolic access to the pore and constitute the main selectivity filter. Modelling approaches based on ar/R signatures were used to predict permeability of plant AQP [12, 13]. For instance, the F-H-T-R signature observed in the PgPIP (Table 2), which seems strictly conserved across PIP from different species, has been associated with water and H_2O_2 permeability [14, 26, 27, 63]. Furthermore, PgPIP1-3 carries the same ar/R motif and similar Froger's residues as OsPIP1-3, which has been recently shown to transport nitrate (NO_3^-) [19]. The H-I-G-R signature observed in PgTIP2-1, PgTIP2-2 and PgTIP2-3, that is conserved in TIP2 from Arabidopsis, maize and rice, supposedly allows permeability to water, NH_3, urea and H_2O_2. The H-I-A-V signature, observed in PgTIP1 (PgTIP1-1), may allow permeability to NH_3, urea and H_2O_2 but restrict water permeability [64–66]. In PgNIP, the W-V-A-R signature have been associated with water, NH_3 and H_2O_2 permeability, while the A-I/A-G/A-R signatures were associated with restricted water and NH_3 permeability. Interestingly, PgNIP2-1 and PgNIP2-2 showed ar/R signatures (G-S-G-R) similar to OsNIP2-1, which is permeable to silicon [18], and also possesses precisely 108 amino-acids between the two NPA motifs, which is assumed to be essential for silicon permeability [67].

Apart from the selectivity filters, a numbers of residues involved in PIP molecular gating mechanisms or subcellular localization were also conserved in PgPIP [8]. For instance, the Histidine (H) on Loop D (H199 in AtPIP2-1), which can be protonated to stabilize the pore in a closed conformation, was conserved in most PgPIP [61, 63, 68]. Furthermore, two Serine residues (S), located on Loop B and C-ter (S121 and S280 in AtPIP2-1) that would favor an open-pore conformation when phosphorylated, were conserved in PgPIP2 [61, 69]. Another Serine residue located on C-ter (S283 in AtPIP2-1), involved in PIP trafficking, was conserved in the PgPIP, with the exception of PgPIP2-7 [70]. Other residues located on the N-ter (Lysine 3 and Glutamate 6 in AtPIP2-1), subjected to methylation and involved in PIP trafficking were also conserved in most PgPIP [71]. Some of these post-translational modification mechanisms can affect aquaporin function in response to particular abiotic or nutritional stimuli and may well be conserved in pearl millet [63, 70, 72, 73].

AQP in plants are expressed in roots and shoots, including inflorescence and pollen. Some PgPIP genes show tissue-specific expression with *PgPIP1-4* and *PgPIP2-3* having higher expression levels in roots, while *PgPIP2-1* is expressed more in shoots and *PgPIP1-1* and *PgPIP1-3* are expressed in both roots and shoots (Fig 5 and S7 Fig). It has been shown that PIP isoforms agglomerate as tetramers in the plasma membrane, each monomer forming functional units. Functional studies as well as protein-protein interactions studies suggest that PIP tetramers can be formed of heteromers of PIP1 and PIP2 with distinct functional properties depending on the isoform combination [74–77]. Based on PgPIP gene expression in pearl millet, PgPIP1-1, PgPIP1-3 and PgPIP1-4 might interact with PgPIP2-3 to form heteromers in roots while PgPIP1-1, PgPIP1-3 and PgPIP2-1 might form different combinations of heteromers in shoots.

Intraspecific diversity in AQP isoform expression has been observed in rice and Arabidopsis [56, 57, 78, 79]. In our study, diversity in expression patterns of PgAQP genes were observed between two pearl millet inbred lines contrasting for water use strategy (Fig 5). IP4952 showed significantly greater AQP contribution to Lpr as compared to IP17150 and also showed significantly higher *PgPIP1-3* and *PgPIP1-4* gene expression. These results suggest

that differences in expression of these AQP genes may reflect differences in AQP contribution to Lpr in pearl millet. These observations are in line with results from [35] showing that the expression of *VvPIP1-1* is associated with root hydraulics and response to water stress in two isohydric and anisohydric grapevine (*Vitis vinifera*) cultivars. Transpiration response to high VPD in four pearl millet recombinant inbred lines has been linked to PgPIP gene expression in roots [31]. The same work suggested that a down-regulation of PgPIP genes under high VPD induced reduction in transpiration and water savings. Our results show lower expression of *PgPIP1-3* and *PgPIP1-4* in IP17150 as well as a reduced role of AQP in Lpr in IP17150, the line with higher water use efficiency. These findings support the observations of [31]. More recently, overexpression of rice OsPIP1-3 enhanced water use efficiency in transgenic tobacco plants [19]. However, this response may well be linked to higher photosynthesis rates due to improved nitrate uptake and transport rather than hydraulics. Overall, expression profiling suggests that APQ may have different physiological functions across the pearl millet plant and contribute to its response to the environment. However, expression alone is certainly not fully representative of AQP function due to various types of post-translational regulations affecting AQP function [8]. Further investigations are needed to better understand the links between reduced transpiration under high VPD, improved water use efficiency and AQP function in roots.

Pearl millet is a drought-adapted crop that will play a major role in the adaptation of agriculture to future climates in arid and semi-arid regions of Africa and India. Here, we provide a comprehensive view of the AQP genes and isoforms present in pearl millet as well as their contribution in root radial water transport. Our results suggest that differential expression of PgPIP1-3 and PgPIP1-4 may be associated with different water use strategies. Therefore, our study supports a potential role of these two AQP isoforms in regulating pearl millet hydraulics and potentially adaptation to challenging environmental conditions.

Supporting information

S1 Table. High scoring pairs with highest bit score at the fifty hot-spots.
(PDF)

S2 Table. Functional annotation of the pearl millet genomic regions corresponding to hot-spots of high scoring pairs.
(PDF)

S3 Table. Primers used for genomic DNA (gDNA) or complementary DNA (cDNA) amplification of aquaporins showing missing sequence.
(PDF)

S4 Table. Primers used for quantitative RT-PCR.
(PDF)

S5 Table. Root architectural traits in IP4952 and IP17150.
(PDF)

S6 Table. Root conductance (L_0), root hydraulic conductivity (Lpr) and aquaporin (AQP) contribution in IP4952 and IP17150.
(PDF)

S7 Table. Analysis of aquaporin conserved domains in pearl millet.
(PDF)

S8 Table. Transmembrane domain analysis of aquaporins in pearl millet.
(PDF)

S1 Fig. Reversion of azide-induced root hydraulic conductivity inhibition.
(PDF)

S2 Fig. Structure of pearl millet aquaporins genes.
(PDF)

S3 Fig. Conserved domains and membrane topology of the TIP isoforms from pearl millet.
(PDF)

S4 Fig. Conserved domains and membrane topology of the NIP isoforms from pearl millet.
(PDF)

S5 Fig. Conserved domains and membrane topology of the SIP isoforms from pearl millet.
(PDF)

S6 Fig. Cavity features of PgPIP isoforms.
(PDF)

S7 Fig. Expression pattern of PgPIP isoforms in shoots of pearl millet.
(PDF)

Acknowledgments

The authors are grateful to Dr Prakash Gangashetty (ICRISAT, Niger) for providing seeds of the inbred lines used in this study, Dr James Burridge (IRD, France) for critical reading and editing of our manuscript and Dr Kwanho Jeong (IRD, France) for his kind support in the preparation of this manuscript. The authors acknowledge the IRD iTrop HPC (South Green Platform) at IRD Montpellier for providing HPC resources that have contributed to the research results reported in this paper (https://bioinfo.ird.fr/- http://www.southgreen.fr).

Author Contributions

Conceptualization: Alexandre Grondin, Christine Tranchant-Dubreuil, Pascal Gantet, Vincent Vadez, Yves Vigouroux, Laurent Laplaze.

Data curation: Alexandre Grondin, Pablo Affortit, Christine Tranchant-Dubreuil, Cédric Mariac.

Formal analysis: Alexandre Grondin, Pablo Affortit, Christine Tranchant-Dubreuil, Cédric Mariac.

Funding acquisition: Vincent Vadez, Yves Vigouroux, Laurent Laplaze.

Investigation: Alexandre Grondin, Pablo Affortit, Christine Tranchant-Dubreuil, Carla de la Fuente-Cantó, Cédric Mariac.

Project administration: Alexandre Grondin, Laurent Laplaze.

Supervision: Alexandre Grondin, Laurent Laplaze.

Writing – original draft: Alexandre Grondin, Laurent Laplaze.

Writing – review & editing: Alexandre Grondin, Christine Tranchant-Dubreuil, Carla de la Fuente-Cantó, Cédric Mariac, Pascal Gantet, Vincent Vadez, Yves Vigouroux, Laurent Laplaze.

References

1. Steudle E. The cohesion-tension mechanism and the acquisition of water by plant roots. Annu Rev Plant Physiol Plant Mol Biol. 2001; 52: 847–875. https://doi.org/10.1146/annurev.arplant.52.1.847 PMID: 11337418
2. Geldner N. The Endodermis. Annu Rev Plant Biol. 2013; 64: 531–558. https://doi.org/10.1146/annurev-arplant-050312-120050 PMID: 23451777
3. Wang P, Calvo-Polanco M, Reyt G, Barberon M, Champeyroux C, Santoni V, et al. Surveillance of cell wall diffusion barrier integrity modulates water and solute transport in plants. Sci Rep. 2019; 9: 1–11. https://doi.org/10.1038/s41598-018-37186-2 PMID: 30626917
4. Abascal F, Irisarri I, Zardoya R. Diversity and evolution of membrane intrinsic proteins. Biochim Biophys Acta. 2014; 1840: 1468–1481. https://doi.org/10.1016/j.bbagen.2013.12.001 PMID: 24355433
5. Verma RK, Gupta AB, Sankararamakrishnan R. Major intrinsic protein superfamily: Channels with unique structural features and diverse selectivity filters. Methods Enzymol. 1st ed. 2015; 557: 485–520. https://doi.org/10.1016/bs.mie.2014.12.006 PMID: 25950979
6. Froger A, Tallur B, Thomas D, Delamarche C. Prediction of functional residues in water channels and related proteins. Protein Sci. 1998; 7: 1458–1468. https://doi.org/10.1002/pro.5560070623 PMID: 9655351
7. Hub JS, De Groot BL. Mechanism of selectivity in aquaporins and aquaglyceroporins. Proc Natl Acad Sci U S A. 2008; 105: 1198–1203. https://doi.org/10.1073/pnas.0707662104 PMID: 18202181
8. Maurel C, Boursiac Y, Luu D-T, Santoni V, Shahzad Z, Verdoucq L. Aquaporins in plants. Physiol Rev. 2015; 95: 1321–58. https://doi.org/10.1152/physrev.00008.2015 PMID: 26336033
9. Ishikawa F, Suga S, Uemura T, Sato MH, Maeshima M. Novel type aquaporin SIPs are mainly localized to the ER membrane and show cell-specific expression in *Arabidopsis thaliana*. FEBS Lett. 2005; 579: 5814–5820. https://doi.org/10.1016/j.febslet.2005.09.076 PMID: 16223486
10. Wudick MM, Luu DT, Maurel C. A look inside: Localization patterns and functions of intracellular plant aquaporins. New Phytol. 2009; 184: 289–302. https://doi.org/10.1111/j.1469-8137.2009.02985.x PMID: 19674338
11. Bienert GP, Bienert MD, Jahn TP, Boutry M, Chaumont F. *Solanaceae* XIPs are plasma membrane aquaporins that facilitate the transport of many uncharged substrates. Plant J. 2011; 66: 306–317. https://doi.org/10.1111/j.1365-313X.2011.04496.x PMID: 21241387
12. Bansal A, Sankararamakrishnan R. Homology modeling of major intrinsic proteins in rice, maize and Arabidopsis: Comparative analysis of transmembrane helix association and aromatic/arginine selectivity filters. BMC Struct Biol. 2007; 7: 1–17. https://doi.org/10.1186/1472-6807-7-1 PMID: 17201922
13. Wallace IS, Roberts DM. Homology modeling of representative subfamilies of Arabidopsis major intrinsic proteins. Classification based on the aromatic/arginine selectivity filter. Plant Physiol. 2004; 135: 1059–1068. https://doi.org/10.1104/pp.103.033415 PMID: 15181215
14. Rodrigues O, Reshetnyak G, Grondin A, Saijo Y, Leonhardt N, Maurel C, et al. Aquaporins facilitate hydrogen peroxide entry into guard cells to mediate ABA- and pathogen-triggered stomatal closure. Proc Natl Acad Sci U S A. 2017;114. https://doi.org/10.1073/pnas.1704754114 PMID: 28784763
15. Uehleln N, Lovisolo C, Siefritz F, Kaldenhoff R. The tobacco aquaporin NtAQP1 is a membrane CO_2 pore with physiological functions. Nature. 2003; 425: 734–737. https://doi.org/10.1038/nature02027 PMID: 14520414
16. Loqué D, Ludewig U, Yuan L, Von Wirén N. Tonoplast intrinsic proteins AtTIP2;1 and AtTIP2;3 facilitate NH_3 transport into the vacuole. Plant Physiol. 2005; 137: 671–680. https://doi.org/10.1104/pp.104.051268 PMID: 15665250
17. Biela A, Grote K, Otto B, Hoth S, Hedrich R, Kaldenhoff R. The *Nicotiana tabacum* plasma membrane aquaporin NtAQP1 is mercury-insensitive and permeable for glycerol. Plant J. 1999; 18: 565–570. https://doi.org/10.1046/j.1365-313x.1999.00474.x PMID: 10417707
18. Ma FJ, Kazunori T, Naoki Y, Namiki M, Saeko K, Maki K, et al. A silicon transporter in rice. Nature. 2006; 440: 688–691. https://doi.org/10.1038/nature04590 PMID: 16572174
19. Liu S, Fukumoto T, Gena P, Feng P, Sun Q, Li Q, et al. Ectopic expression of a rice plasma membrane intrinsic protein (OsPIP1;3) promotes plant growth and water uptake. Plant J. 2020; 102: 779–796. https://doi.org/10.1111/tpj.14662 PMID: 31872463
20. Chaumont F, Barrieu F, Wojcik E, Chrispeels MJ, Jung R. Aquaporins constitute a large and highly divergent protein family in maize. Plant Physiol. 2001; 125: 1206–1215. https://doi.org/10.1104/pp.125.3.1206 PMID: 11244102
21. Azad AK, Ahmed J, Md Asraful A, Md Mahbub H, Ishikawa T, Sawa Y, et al. Genome-wide characterization of major intrinsic proteins in four grass plants and their non-aqua transport selectivity profiles with

comparative perspective. PLoS One. 2016; 11: e0157735. https://doi.org/10.1371/journal.pone.0157735 PMID: 27327960

22. Reddy PS, Rao TSRB, Sharma KK, Vadez V. Genome-wide identification and characterization of the aquaporin gene family in *Sorghum bicolor* (L.). Plant Gene. 2015; 1: 18–28. https://doi.org/10.1016/j.plgene.2014.12.002

23. Sakurai J, Ishikawa F, Yamaguchi T, Uemura M, Maeshima M. Identification of 33 rice aquaporin genes and analysis of their expression and function. Plant Cell Physiol. 2005; 46: 1568–77. https://doi.org/10.1093/pcp/pci172 PMID: 16033806

24. Guerriero G, Deshmukh R, Sonah H, Sergeant K, Hausman JF, Lentzen E, et al. Identification of the aquaporin gene family in *Cannabis sativa* and evidence for the accumulation of silicon in its tissues. Plant Sci. 2019; 287: 110167. https://doi.org/10.1016/j.plantsci.2019.110167 PMID: 31481224

25. Reuscher S, Akiyama M, Mori C, Aoki K, Shibata D, Shiratake K. Genome-wide identification and expression analysis of aquaporins in tomato. PLoS One. 2013; 8: e79052. https://doi.org/10.1371/journal.pone.0079052 PMID: 24260152

26. Javot H, Lauvergeat V, Santoni V, Martin-Laurent F, Güçlü J, Vinh J, et al. Role of a single aquaporin isoform in root water uptake. Plant Cell. 2003; 15: 509–522. https://doi.org/10.1105/tpc.008888 PMID: 12566588

27. Postaire O, Tournaire-Roux C, Grondin A, Boursiac Y, Morillon R, Schäffner AR, et al. A PIP1 aquaporin contributes to hydrostatic pressure-induced water transport in both the root and rosette of Arabidopsis. Plant Physiol. 2010; 152: 1418–1430. https://doi.org/10.1104/pp.109.145326 PMID: 20034965

28. Vadez V. Root hydraulics: The forgotten side of roots in drought adaptation. F Crop Res. 2014; 165: 15–24. https://doi.org/10.1016/j.fcr.2014.03.017

29. Moshelion M, Halperin O, Wallach R, Oren R, Way DA. Role of aquaporins in determining transpiration and photosynthesis in water-stressed plants: Crop water-use efficiency, growth and yield. Plant, Cell Environ. 2015; 38: 1785–1793. https://doi.org/10.1111/pce.12410 PMID: 25039365

30. Shekoofa A, Sinclair T. Aquaporin activity to improve crop drought tolerance. Cells. 2018; 7: 123. https://doi.org/10.3390/cells7090123 PMID: 30158445

31. Reddy PS, Tharanya M, Sivasakthi K, Srikanth M, Hash CT, Kholova J, et al. Molecular cloning and expression analysis of aquaporin genes in pearl millet [*Pennisetum glaucum* (L) R. Br.] genotypes contrasting in their transpiration response to high vapour pressure deficits. Plant Sci. 2017; 265: 167–176. https://doi.org/10.1016/j.plantsci.2017.10.005 PMID: 29223338

32. Zhang C, Postma JA, York LM, Lynch JP. Root foraging elicits niche complementarity-dependent yield advantage in the ancient 'three sisters' (maize/bean/squash) polyculture. Ann Bot. 2014; 114: 1719–1733. https://doi.org/10.1093/aob/mcu191 PMID: 25274551

33. Tharanya M, Kholova J, Sivasakthi K, Seghal D, Hash CT, Raj B, et al. Quantitative trait loci (QTLs) for water use and crop production traits co-locate with major QTL for tolerance to water deficit in a fine-mapping population of pearl millet (*Pennisetum glaucum* L. R.Br.). Theor Appl Genet. 2018; 131: 1509–1529. https://doi.org/10.1007/s00122-018-3094-6 PMID: 29679097

34. Sadok W, Sinclair TR. Transpiration response of "slow-wilting" and commercial soybean (*Glycine max* (L.) Merr.) genotypes to three aquaporin inhibitors. J Exp Bot. 2010; 61: 821–829. https://doi.org/10.1093/jxb/erp350 PMID: 19969533

35. Vandeleur RK, Mayo G, Shelden MC, Gilliham M, Kaiser BN, Tyerman SD. The role of plasma membrane intrinsic protein aquaporins in water transport through roots: Diurnal and drought stress responses reveal different strategies between isohydric and anisohydric cultivars of grapevine. Plant Physiol. 2009; 149: 445–460. https://doi.org/10.1104/pp.108.128645 PMID: 18987216

36. Sakurai-Ishikawa J, Murai-Hatano M, Hayashi H, Ahamed A, Fukushi K, Matsumoto T, et al. Transpiration from shoots triggers diurnal changes in root aquaporin expression. Plant, Cell Environ. 2011; 34: 1150–1163. https://doi.org/10.1111/j.1365-3040.2011.02313.x PMID: 21414014

37. Sade N, Vinocur BJ, Diber A, Shatil A, Ronen G, Nissan H, et al. Improving plant stress tolerance and yield production: Is the tonoplast aquaporin SiTIP2;2 a key to isohydric to anisohydric conversion? New Phytol. 2009; 181: 651–661. https://doi.org/10.1111/j.1469-8137.2008.02689.x PMID: 19054338

38. Kholová J, Hash CT, Kakkera A, Koová M, Vadez V. Constitutive water-conserving mechanisms are correlated with the terminal drought tolerance of pearl millet [*Pennisetum glaucum* (L.) R. Br.]. J Exp Bot. 2010; 61: 369–377. https://doi.org/10.1093/jxb/erp314 PMID: 19861657

39. Kholová J, Nepolean T, Tom Hash C, Supriya A, Rajaram V, Senthilvel S, et al. Water saving traits co-map with a major terminal drought tolerance quantitative trait locus in pearl millet [*Pennisetum glaucum* (L.) R. Br.]. Mol Breed. 2012; 30: 1337–1353. https://doi.org/10.1007/s11032-012-9720-0

40. Vadez V, Kholova J, Zaman-Allah M, Belko N. Water: The most important "molecular" component of water stress tolerance research. Funct Plant Biol. 2013; 40: 1310–1322. https://doi.org/10.1071/FP13149 PMID: 32481197

41. Debieu M, Kanfany G, Laplaze L. Pearl millet genome: Lessons from a tough crop. Trends Plant Sci. 2017; 22: 911–913. https://doi.org/10.1016/j.tplants.2017.09.006 PMID: 28939172

42. Sultan B, Defrance D, Iizumi T. Evidence of crop production losses in West Africa due to historical global warming in two crop models. Sci Rep. 2019; 9: 1–15. https://doi.org/10.1038/s41598-018-37186-2 PMID: 30626917

43. Debieu M, Sine B, Passot S, Grondin A, Akata E, Gangashetty P, et al. Response to early drought stress and identification of QTLs controlling biomass production under drought in pearl millet. PLoS One. 2018; 13: 1–19. https://doi.org/10.1371/journal.pone.0201635 PMID: 30359386

44. Varshney RK, Shi C, Thudi M, Mariac C, Wallace J, Qi P, et al. Pearl millet genome sequence provides a resource to improve agronomic traits in arid environments. Nat Biotechnol. 2017; 35: 969–976. https://doi.org/10.1038/nbt.3943 PMID: 28922347

45. Vadez V, Deshpande SP, Kholova J, Hammer GL, Borrell AK, Talwar HS, et al. Stay-green quantitative trait loci's effects on water extraction, transpiration efficiency and seed yield depend on recipient parent background. Funct Plant Biol. 2011; 131: 1509–1529. https://doi.org/10.1071/FP11073 PMID: 32480908

46. Vadez V, Kholova J, Medina S, Kakkera A, Anderberg H. Transpiration efficiency: New insights into an old story. J Exp Bot. 2014; 65: 6141–6153. https://doi.org/10.1093/jxb/eru040 PMID: 24600020

47. Hoagland DR, Arnon DI. The water-culture method for growing plants without soil. Calif Agr Expt Sta Circ. 1950; 347: 1–32. citeulike-article-id:9455435

48. Boursiac Y, Chen S, Luu D-T, Sorieul M, van den Dries N, Maurel C. Early effects of salinity on water transport in Arabidopsis roots. Molecular and cellular features of aquaporin expression. Plant Physiol. 2005; 139: 790–805. https://doi.org/10.1104/pp.105.065029 PMID: 16183846

49. Henry A, Cal AJ, Batoto TC, Torres RO, Serraj R. Root attributes affecting water uptake of rice (*Oryza sativa*) under drought. J Exp Bot. 2012; 63: 4751–4763. https://doi.org/10.1093/jxb/ers150 PMID: 22791828

50. Sarah G, Homa F, Pointet S, Contreras S, Sabot F, Nabholz B, et al. A large set of 26 new reference transcriptomes dedicated to comparative population genomics in crops and wild relatives. Mol Ecol Resour. 2017; 17: 565–580. https://doi.org/10.1111/1755-0998.12587 PMID: 27487989

51. Milne I, Stephen G, Bayer M, Cock PJA, Pritchard L, Cardle L, et al. Using tablet for visual exploration of second-generation sequencing data. Brief Bioinform. 2013; 14: 193–202. https://doi.org/10.1093/bib/bbs012 PMID: 22445902

52. Hu B, Jin J, Guo AY, Zhang H, Luo J, Gao G. GSDS 2.0: An upgraded gene feature visualization server. Bioinformatics. 2015; 15: 1296–1297. https://doi.org/10.1093/bioinformatics/btu817 PMID: 25504850

53. Kelley LA, Mezulis S, Yates CM, Wass MN, Sternberg MJE. The Phyre2 web portal for protein modeling, prediction and analysis. Nat Protoc. 2015; 10: 845. https://doi.org/10.1038/nprot.2015.053 PMID: 25950237

54. Kumar S, Stecher G, Tamura K. MEGA7: Molecular Evolutionary Genetics Analysis version 7.0 for bigger datasets. Mol Biol Evol. 2016; 33: 1870–1874. https://doi.org/10.1093/molbev/msw054 PMID: 27004904

55. Javot H, Maurel C. The role of aquaporins in root water uptake. Ann Bot. 2002; 90: 301–313. https://doi.org/10.1093/aob/mcf199 PMID: 12234142

56. Sutka M, Li G, Boudet J, Boursiac Y, Doumas P, Maurel C. Natural variation of root hydraulics in Arabidopsis grown in normal and salt-stressed conditions. Plant Physiol. 2011; 155: 1264–1276. https://doi.org/10.1104/pp.110.163113 PMID: 21212301

57. Grondin A, Mauleon R, Vadez V, Henry A. Root aquaporins contribute to whole plant water fluxes under drought stress in rice (*Oryza sativa* L.). Plant, Cell Environ. 2016;39. https://doi.org/10.1111/pce.12616 PMID: 26226878

58. Johanson U, Karlsson M, Johansson I, Gustavsson S, Sjövall S, Fraysse L, et al. The complete set of genes encoding major intrinsic proteins in Arabidopsis provides a framework for a new nomenclature for major intrinsic proteins in plants. Plant Physiol. 2001; 126: 1358–1369. https://doi.org/10.1104/pp.126.4.1358 PMID: 11500536

59. Tattini L, D'Aurizio R, Magi A. Detection of genomic structural variants from next-generation sequencing data. Front Bioeng Biotechnol. 2015; 25: 3–92. https://doi.org/10.3389/fbioe.2015.00092 PMID: 26161383

60. Chakrabarti N, Tajkhorshid E, Roux B, Pomès R. Molecular basis of proton blockage in aquaporins. Structure. 2004; 12: 65–74. https://doi.org/10.1016/j.str.2003.11.017 PMID: 14725766

61. Törnroth-Horsefield S, Wang Y, Hedfalk K, Johanson U, Karlsson M, Tajkhorshid E, et al. Structural mechanism of plant aquaporin gating. Nature. 2006; 439: 688–694. https://doi.org/10.1038/nature04316 PMID: 16340961

62. Mori IC, Rhee J, Shibasaka M, Sasano S, Kaneko T, Horie T, et al. CO_2 transport by PIP2 aquaporins of barley. Plant Cell Physiol. 2014; 55: 251–257. https://doi.org/10.1093/pcp/pcu003 PMID: 24406630

63. Tournaire-Roux C, Sutka M, Javot H, Gout E, Gerbeau P, Luu D-T, et al. Cytosolic pH regulates root water transport during anoxic stress through gating of aquaporins. Nature. 2003; 425: 393–397. https://doi.org/10.1038/nature01853 PMID: 14508488

64. Maurel C, Reizer J, Schroeder JI, Chrispeels MJ. The vacuolar membrane protein gamma-TIP creates water specific channels in *Xenopus* oocytes. EMBO J. 1993; 12: 2241–2247. https://doi.org/10.1002/j.1460-2075.1993.tb05877.x PMID: 8508761

65. Dynowski M, Schaaf G, Loque D, Moran O, Ludewig U. Plant plasma membrane water channels conduct the signalling molecule H_2O_2. Biochem J. 2008; 414: 53–61. https://doi.org/10.1042/BJ20080287 PMID: 18462192

66. Jahn TP, Møller ALB, Zeuthen T, Holm LM, Klærke DA, Mohsin B, et al. Aquaporin homologues in plants and mammals transport ammonia. FEBS Lett. 2004; 574: 31–36. https://doi.org/10.1016/j.febslet.2004.08.004 PMID: 15358535

67. Deshmukh RK, Vivancos J, Ramakrishnan G, Guérin V, Carpentier G, Sonah H, et al. A precise spacing between the NPA domains of aquaporins is essential for silicon permeability in plants. Plant J. 2015; 83: 489–500. https://doi.org/10.1111/tpj.12904 PMID: 26095507

68. Verdoucq L, Grondin A, Maurel C. Structure-function analysis of plant aquaporin AtPIP2;1 gating by divalent cations and protons. Biochem J. 2008; 415: 409–416. https://doi.org/10.1042/BJ20080275 PMID: 18637793

69. Johansson I, Karlsson M, Shukla VK, Chrispeels MJ, Larsson C, Kjellbom P. Water transport activity of plasma membrane aquaporin PM28A is regulated by phosphorylation. Plant Cell. 1998; 10: 451–459. https://doi.org/10.1105/tpc.10.3.451 PMID: 9501117

70. Prak S, Hem S, Boudet J, Viennois G, Sommerer N, Rossignol M, et al. Multiple phosphorylations in the C-terminal tail of plant plasma membrane aquaporins: Role in subcellular trafficking of AtPIP2;1 in response to salt stress. Mol Cell Proteomics. 2008; 7: 1019–1030. https://doi.org/10.1074/mcp.M700566-MCP200 PMID: 18234664

71. Santoni V, Verdoucq L, Sommerer N, Vinh J, Pflieger D, Maurel C. Methylation of aquaporins in plant plasma membrane. Biochem J. 2006; 400: 189–197. https://doi.org/10.1042/BJ20060569 PMID: 16839310

72. Grondin A, Rodrigues O, Verdoucq L, Merlot S, Leonhardt N, Maurel C. Aquaporins contribute to ABA-triggered stomatal closure through OST1-mediated phosphorylation. Plant Cell. 2015;27. https://doi.org/10.1105/tpc.15.00421 PMID: 26163575

73. di Pietro M, Vialaret J, Li G-W, Hem S, Prado K, Rossignol M, et al. Coordinated post-translational responses of aquaporins to abiotic and nutritional stimuli in Arabidopsis roots. Mol Cell proteomics. 2013; 12: 3886–97. https://doi.org/10.1074/mcp.M113.028241 PMID: 24056735

74. Fetter K, Van Wilder V, Moshelion M, Chaumont F. Interactions between plasma membrane aquaporins modulate their water channel activity. Plant Cell. 2004; 16: 215–228. https://doi.org/10.1105/tpc.017194 PMID: 14671024

75. Zelazny E, Borst JW, Muylaert M, Batoko H, Hemminga MA, Chaumont F. FRET imaging in living maize cells reveals that plasma membrane aquaporins interact to regulate their subcellular localization. Proc Natl Acad Sci U S A. 2007; 104: 12359–12364. https://doi.org/10.1073/pnas.0701180104 PMID: 17636130

76. Yaneff A, Sigaut L, Marquez M, Alleva K, Pietrasanta LI, Amodeo G. Heteromerization of PIP aquaporins affects their intrinsic permeability. Proc Natl Acad Sci U S A. 2014; 111: 231–236. https://doi.org/10.1073/pnas.1316537111 PMID: 24367080

77. Bellati J, Alleva K, Soto G, Vitali V, Jozefkowicz C, Amodeo G. Intracellular pH sensing is altered by plasma membrane PIP aquaporin co-expression. Plant Mol Biol. 2010; 74: 105–118. https://doi.org/10.1007/s11103-010-9658-8 PMID: 20593222

78. Lian H-L, Yu X, Lane D, Sun W-N, Tang Z-C, Su W-A. Upland rice and lowland rice exhibited different PIP expression under water deficit and ABA treatment. Cell Res. 2006; 16: 651–60. https://doi.org/10.1038/sj.cr.7310068 PMID: 16773042

79. Alexandersson E, Danielson JÅH, Råde J, Moparthi VK, Fontes M, Kjellbom P, et al. Transcriptional regulation of aquaporins in accessions of Arabidopsis in response to drought stress. Plant J. 2010; 61: 650–660. https://doi.org/10.1111/j.1365-313X.2009.04087.x PMID: 19947979